Soccer games and record-breaking PM$_{2.5}$ pollution events in Santiago, Chile.

Rémy Lapere[1], Laurent Menut[1], Sylvain Mailler[1,2], and Nicolás Huneeus[3,4]

[1]LMD/IPSL, École Polytechnique, Institut Polytechnique de Paris, ENS, PSL Université, Sorbonne Université, CNRS, Palaiseau, France
[2]Ecole des Ponts, Marne-la-Vallée, France
[3]Universidad de Chile, Santiago, Chile
[4]Center for Climate and Resilience Research CR2, Universidad de Chile, Santiago, Chile

Correspondence: Rémy Lapere (remy.lapere@lmd.polytechnique.fr)

Abstract. In wintertime, high concentrations of atmospheric fine particulate matter (PM$_{2.5}$) are commonly observed in the metropolitan area of Santiago, Chile. Hourly peaks can be very strong, up to ten times above average levels, but have barely been studied so far. Based on atmospheric composition measurements and chemistry-transport modeling (WRF-CHIMERE), the chemical signature of sporadic skyrocketing wintertime PM$_{2.5}$ peaks is analyzed. This signature and the timing of such extreme events traces their origin back to massive barbecue cooking by Santiago's inhabitants during international soccer games. The peaks end up evacuated outside Santiago after a few hours but trigger emergency plans for the next day. Decontamination plans in Santiago focus on decreasing traffic, industrial and residential heating emissions. Thanks to the air quality network of Santiago, this study shows that cultural habits such as barbecue cooking also need to be taken into account. For short-term forecast and emergency management, cultural events such as soccer games seem a good proxy to prognose possible PM$_{2.5}$ peak events. Not only this result can have an informative value for the Chilean authorities, but a similar methodology could also be reproduced for other cases throughout the world in order to estimate the burden on air quality of cultural habits.

1 Introduction

Santiago, the capital city of Chile (33.5°S, 70.5°W, 570m a.s.l.) regularly faces high levels of fine particulate matter (PM$_{2.5}$) pollution in winter. The city is located in a confined geographical basin surrounded by the Andes cordillera in the East, a coastal range in the West, and transversal mountain chains in the South and North (Rutllant and Garreaud, 1995). The induced poor ventilation in wintertime combined with significant anthropogenic emissions lead to high average levels of PM$_{2.5}$ (Barraza et al., 2017; Mazzeo et al., 2018) as well as peak events (Toro A et al., 2018). Hourly surface concentrations can reach up to 600μg/m^3 in the Western part of the city according to the local air quality monitoring network. Between June and July 2016 records show that the station of Pudahuel saw only seven days with an average PM$_{2.5}$ concentration below the 25μg/m^3

24-hour mean standard defined by the World Health Organization (World Health Organization, 2006). 7 million people live in the metropolitan area and are exposed to such atmospheric pollution. The associated life expectancy reduction caused by $PM_{2.5}$ inhalation ranks Chile among the countries with air pollution issues (Energy Policy Institute at the University of Chicago, 2017). In this respect, atmospheric decontamination plans were designed by local authorities in the recent years (Gallardo et al., 2018; Ministerio del Medio Ambiente, 2012). However the source and impacts of extreme peak events as well as the benefits of their mitigation are relatively unknown.

Several studies have been conducted to improve the $PM_{2.5}$ concentration forecast system in Santiago (Rutllant and Garreaud, 1995; Saide et al., 2016; Mazzeo et al., 2018). However, none of them describe the sharp sporadic peaks observed some years in June and July nor explain their origin, while their impact is substantial. Acute health effects of strong, time-limited $PM_{2.5}$ events are known to be significant in Santiago, with increases in respiratory emergency and pneumonia visits within 2 days after such a peak (Ilabaca et al., 2011). Government reports also provide evidence that highly polluted conditions affect the local economy, and estimate the net benefit of compliance with PM standards to several millions of US dollars (Ministerio del Medio Ambiente, 2012). This study combines the automated air quality monitoring network of Santiago and chemistry-transport modeling to describe and identify the source of recent short-lived $PM_{2.5}$ extreme events occurring in wintertime. The dispersion pattern of such events in June 2016 is also modeled.

Section 2 presents the data and model configuration used in this study. Section 3 describes the outcomes of both the data analysis and the chemistry-transport simulations regarding the identification of the origin of the extreme events considered. Section 4 discusses the hypotheses underlying the conclusions, which are detailed in Section 5.

2 Data and methods

2.1 Observation data

Time series of hourly surface measurements of meteorology and air quality are extracted from the automated air quality monitoring network of Santiago (SINCA - https://sinca.mma.gob.cl/index.php/region/index/id/M). The distribution of these urban air quality monitoring stations can be seen in Fig. 4 for instance. This network uses beta ray attenuation technology (Met One Instruments' Model BAM-1020) for $PM_{2.5}$ concentrations measurements, gas-phase chemiluminescence (Thermo Scientific Model 42i) for NO_X, and infrared photometry by gas filter correlation (Thermo Scientific Model 48i) for CO. Vertical meteorological profiles used for the validation of the simulations were provided by the Dirección Meteorológica de Chile. Ceilometer back-scattering profiles were measured and provided by the University of Chile.

2.2 Model set-up

The chemistry-transport simulations are based on the combination of WRF mesoscale weather numerical model, HTAP anthropogenic emissions inventory and CHIMERE chemistry-transport model. The simulation domains are described in Fig. 1, with a coarse domain at 15km spatial resolution comprising most of Chile, and a nested domain focusing on central Chile and

centered on Santiago at 3km resolution. The meteorological conditions are simulated using the Weather Research and Fore-casting model from the US National Center for Atmospheric Research (Skamarock et al., 2008). The model configuration used in this study to simulate and reproduce observed meteorological conditions are presented in Table 1. The model was applied to
55 46 vertical levels up to the highest elevation of 50hPa, in a two-way nested fashion, with 1-2-1 smoothing. Initial and boundary conditions used are FNL analysis, with a 1° by 1° spatial resolution and 6-hour temporal resolution, from the Global Forecast System (NCEP, 2000). Land-use and orography are based on the modified IGBP MODIS 20-category database with 30sec res-olution (University of Maryland, 2010). The simulated period is June 1ˢᵗ to July 15ᵗʰ 2016. The starting period from June 1ˢᵗ to June 15ᵗʰ is used for spin-up and will not be analyzed. CHIMERE is an Eulerian 3-dimensional regional Chemistry-Transport
60 Model, able to reproduce gas-phase chemistry, aerosols formation, transport and deposition. In this study the 2017 off-line version of CHIMERE is used (Mailler et al., 2017). The configuration used for this study is described in Table 1. Land-use and orography data is the same as for WRF. For anthropogenic emissions, the HTAP V2 dataset is used which consists of 0.1° gridded maps of air pollutant emissions for the year 2010 (Janssens-Maenhout et al., 2015). A downscaling is applied to this inventory based on land-use and demographics characteristics, and monthly emissions are split in time down to daily/hourly
65 rates following the methodology of (Menut et al., 2013).
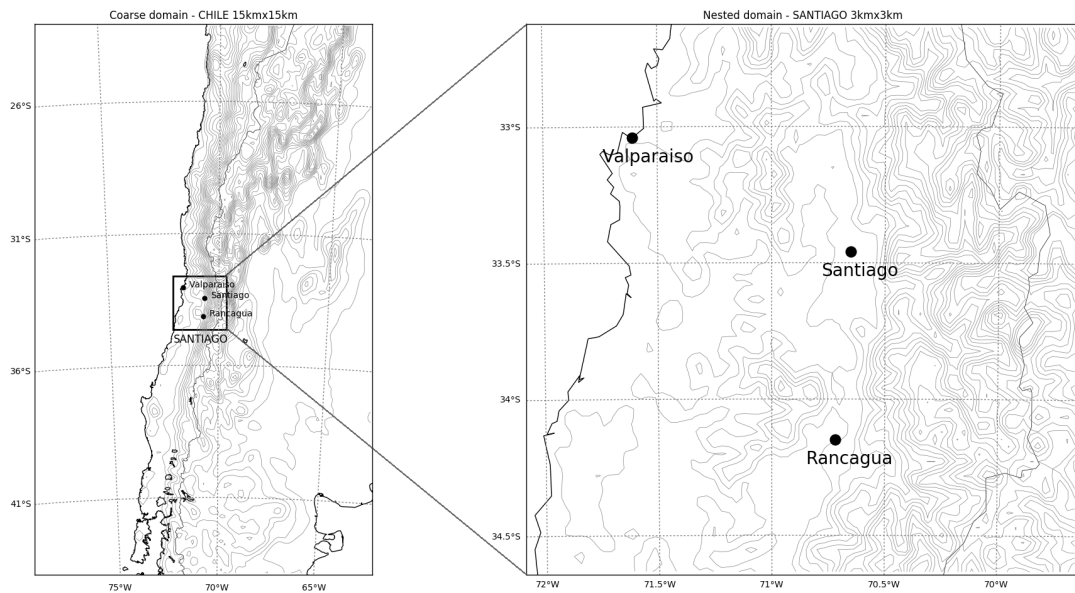
Figure 1. Left: coarse simulation domain at 15km resolution. Right: nested domain at 3km resolution. 250m contour levels shown are interpolated from the modified IGBP MODIS 20-category database with 30sec resolution (University of Maryland, 2010).

2.3 Simulation validation

Simulation scores are gathered in Tables 2, 3 and 4. Two stations downtown are used to validate the simulated near-surface me-teorology - Table 2. Biases (MB) for temperature are around +/-1°C with correlations (R) around 0.85. The model is a little too

70 dry with relative humidity biases between -12% and -16% but mostly reproduces the diurnal cycle with correlations of 0.62 and 0.7. 10m wind speed time series is fairly well reproduced with mean biases of -0.08m/s (8%) and 0.23m/s (32%) respectively for observed average values of 1.04m/s and 0.70m/s, and correlations of 0.56 and 0.7. Vertical meteorological profiles scores are shown in Table 3. For the three days presented the statistics are satisfactory. Typical daily average concentrations of $PM_{2.5}$ are quite well reproduced by the model. Table 4 gathers the scores for $PM_{2.5}$ for some stations, between June 28th and July 15th

75 so as to avoid the peaks that do not represent business as usual conditions. Mean biases are less than $5\mu g/m^3$ to be compared with average hourly levels over the period between $35\mu g/m^3$ and $55\mu g/m^3$ for these stations. Corresponding correlations are between 0.45 and 0.63, which are decent values. The representation of wind by the model for synoptic meteorological stations in Santiago, is described in Table 3 and Fig. 2. Generally speaking the model behaves well for 10m values and profiles of wind speed and direction, so that transport should be realistically represented.
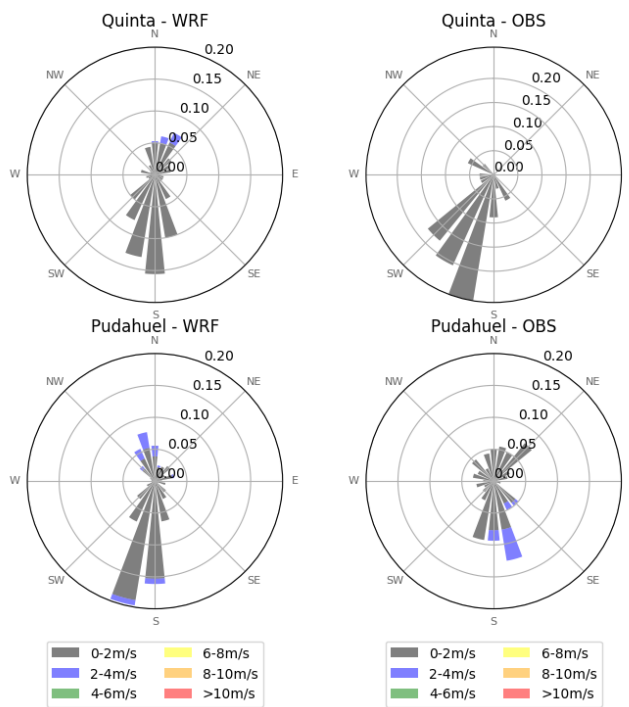
Figure 2. Modeled (left) and observed (right) wind rose between June 15th and 30th 2016 - synoptic stations Pudahuel and Quinta Normal

80 The modeling setup is based on WRF-CHIMERE, with a horizontal resolution of 3km, and emissions are downscaled from a dataset originally at a 0.1° resolution. At the scale of a city such as Santiago, which is roughly 20km by 20km, such a resolution might seem too coarse to capture the observed heterogeneity. However, the previous analysis shows that the meteorological conditions are well reproduced by the model, and the spatial distribution of $PM_{2.5}$ concentrations also accounts for the observed heterogeneity (see Fig. 10 for instance). Mazzeo et al. (2018) used a similar setup with a 2km resolution for a sensitivity analysis

85 to traffic and residential heating emissions in Santiago, yielding similar performances. Comparable CHIMERE simulations are

performed for purposes of air quality operational forecast in France, which performance at small scale is acknowledged in the literature, provided emissions have appropriate magnitudes (Petit et al., 2017; Shaiganfar et al., 2017).

3   Results

3.1   PM$_{2.5}$ peaks description

90   The following analysis is based on the data provided by the "Sistema de Información Nacional de Calidad del Aire" (SINCA) network of surface air quality sensors distributed in the metropolitan area of Santiago (Ministerio del Medio Ambiente, 2018). The time series of PM$_{2.5}$ concentrations for each of the 11 stations of this network for June and July 2016 are illustrated in Fig. 3. Two skyrocketing peaks, up to ten times higher than the average concentration for the season, occurred at several stations during the nights between June 18th/19th and 26th/27th. These two peaks reached all-time record breaking levels for

95   some stations in the city according to the available SINCA time series. Other stations show less extreme peaks, which is representative of the rich dynamics of particulate matter within Santiago (Toledo et al., 2018). Understanding the origin and modeling the dispersion of these time-limited, very sharp events is the purpose of this study. For the following analysis, the peak on June 26th/27th is considered, although the analysis and results are the same for June 18th/19th. Its spatial evolution can be found in Fig. 4, showing that the episode starts simultaneously at several air quality stations at around 8pm, levels decreasing

100   back to regular values the next morning. The Western part of the city seems much more affected by the event than the Eastern part. This comes from the diurnal wind cycle in Santiago, that features prevailing easterlies during night time contributing to renew air masses in this part of the city (Rutllant and Garreaud, 1995).
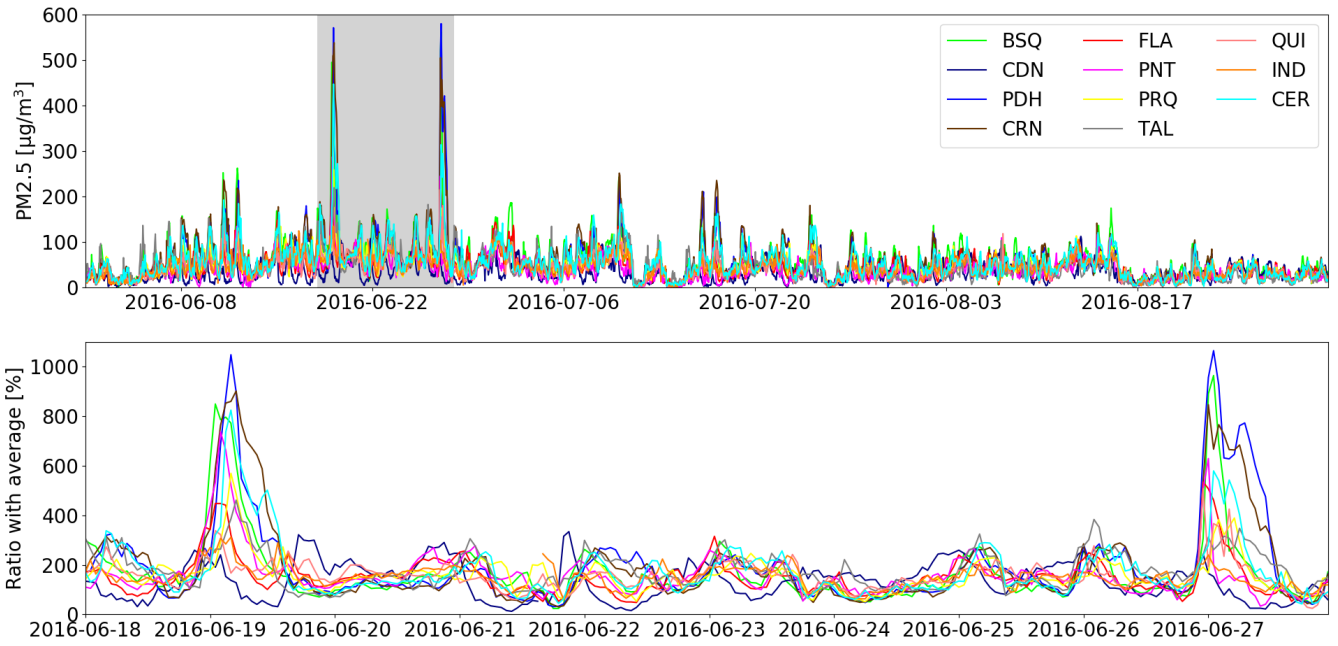
Figure 3. Top: time series of hourly PM$_{2.5}$ concentration between June 1st and August 31st 2016 for the 11 stations of the air quality network of Santiago. Bottom: ratio between hourly PM$_{2.5}$ and average over the summer, zoomed between June 18th and June 28th (shaded period in top graph).
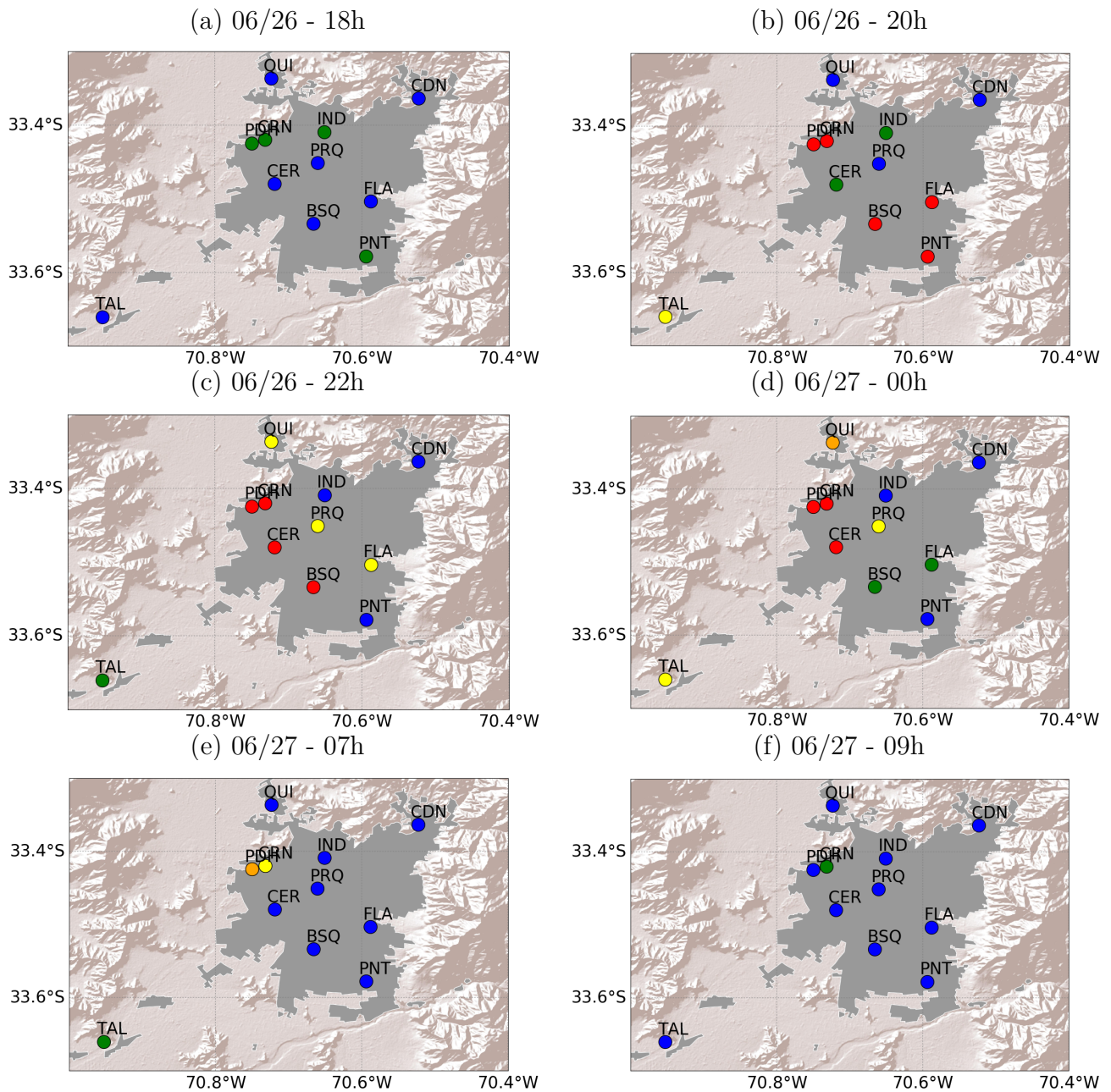
Figure 4. Observed PM$_{2.5}$ hourly concentrations during the peak on June 26thcompared to its average over summer 2016 - blue <= 200%, green <= 300%, yellow <= 400%, orange <= 500%, red >500%. Map background layer: World Shaded Relief, ©2009 ESRI.

The meteorological conditions observed at the location of the strongest peak during our period of interest are shown in Fig. 5. Red lines correspond to the measurements between June 26th 6 a.m. and June 27th 5 a.m. (local time) which comprises a peak

105 event. Figures 5a and 5b show that at the location of the strongest PM$_{2.5}$ peak, the surface temperature and relative humidity cycles over the duration of the event are very close to the average over the month (black line). Wind speed - Fig. 5c - is a little slower than average on the whole but remains in the range of the 1st and 3rd quartiles of ventilation conditions (dashed white lines). Ceilometer profiles and boundary layer height (BLH) estimation based on the methods from (Muñoz and Undurraga, 2010) derived for each day at 3 p.m. - white diamonds in Fig. 5d - indicate that the mixed layer is rather shallow around the

110 peak but not shallower than on the 22nd/23rd for instance, which did not feature such an event. On June 26th, the mixed layer is 430m high, which is close to the average height over the period, and much higher than the minimum value (260m) obtained on June 21st.
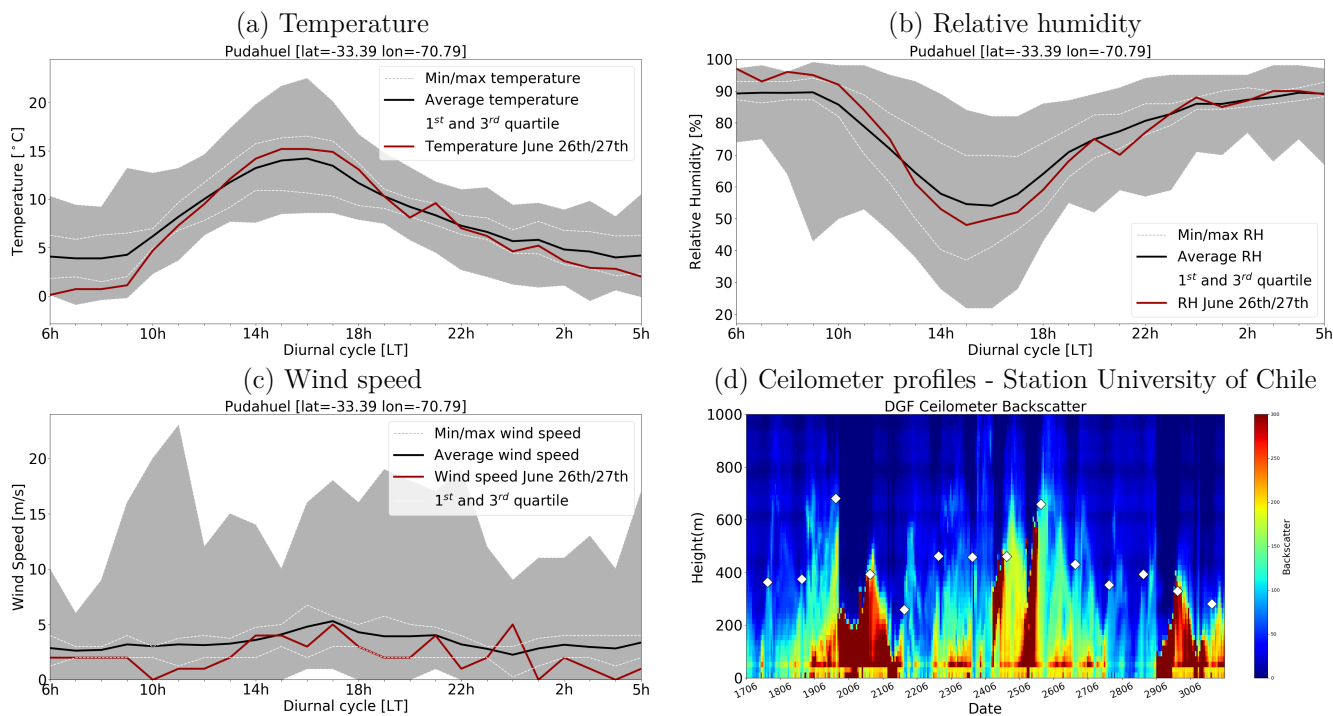
Figure 5. Meteorological conditions around June 26th/27th PM$_{2.5}$ episode for the synoptic station Pudahuel. (a),(b),(c) average (black line), minima and maxima (gray area), 25% and 75% quantiles (white dashed line) between June 15th and July 15th 2016. The red lines show the values for June 26th 6 a.m. to June 27th 5 a.m. (d) hourly backscatter profiles from June 17th through June 30th 2016 and mixed layer height at 3 p.m. (white diamond markers).

Hence, measurements show that the meteorological conditions during the peak are not very different from other days of the period, when no PM peak was recorded. Thus, meteorological conditions are not to consider as the main forcing for the PM$_{2.5}$

115 event although they are favorable for it to appear, which is usual for the season in the area of Santiago.

Besides meteorology, advection of a PM plume over the city could be a candidate cause for such events. For instance, wildfires occurring in the forests surrounding the city occasionally explain major peaks of particulate matter in Santiago

(Rubio et al., 2015; de la Barrera et al., 2018), but these events mostly take place in austral summer, and no such event was reported during our period of study. In addition, the strong concentration gradients observed between nearby stations (Fig. 3 and 4) makes advection unlikely responsible for these events.

Once meteorology and transport are ruled out as root causes, high local emissions must then be underlying the very strong concentrations recorded.

3.2 Chemical signature and source identification

In order to identify the type of source involved in the sporadic peaks, Fig. 7 shows a scatter plot of $PM_{2.5}$, NO_X and CO hourly surface concentrations from June 15th to June 30th 2016, for Pudahuel air quality station. Red dots correspond to $PM_{2.5}$ concentrations higher than $200 \mu g/m^3$, blue dots to concentrations below that value. Out of simplicity, from now on we will refer to the former as PPE (PM peak events) and to the latter as PRS (PM regular situation). Two different regimes can be identified: for PPE, the NO_X/CO ratio is around 4.6%, while for PRS, it is approximately 14%. The same goes for the $NO_X/PM_{2.5}$ ratio, with values around 73% for PPE, and 502% otherwise. Given the short-lived character of the events considered, such different concentration ratios can be related to different emission factors as discussed in Sect. 4. Thus, two different types of source are involved in the two situations (PPE/PRS) considered.

(Mazzeo et al., 2018) found a $NO_X/PM_{2.5}$ ratio of 526% for Pudahuel station in July 2015, without peak events. Using the same methodology and combining data from July 2015 and 2016, without peak events, we recover a concentration ratio around 557% for this same station. For NO_X/CO we find it is around 14% (see Fig. 6). These two values correspond to the average pollution situation in this part of the city, i.e. what is usually observed in wintertime when no peak event occurs. They are comparable to what can be observed in PRS in Fig. 7 with an average ratio of 502% for $NO_X/PM_{2.5}$ and 14% for NO_X/CO. Therefore, the PM regular situation (PRS) fairly corresponds to the average situation in Santiago in winter. Peak events (PPE - red dots) however show very different ratios that do not coincide with the average situation, hence pointing to another specific source. Major contributors to atmospheric pollution in Santiago are traffic (39%), industry (18%) and residential heating (20%) (Barraza et al., 2017). Based on the current EURO 5 legislation for car engines emissions in place in Chile (Ministerio del Medio Ambiente, 2017) and the vehicles fleet in Santiago (Instituto Nacional de Estadísticas, 2016), the expected emission ratio from traffic yields around 12% for NO_X/CO and 1680% for $NO_X/PM_{2.5}$. Similarly, emission ratios extracted from the HTAP inventory for traffic at the grid point corresponding to Santiago yield 7.5% for NO_X/CO and 1750% for $NO_X/PM_{2.5}$. This does not match with the PPE signal, especially regarding NO_X and $PM_{2.5}$. For residential heating, the HTAP inventory gives emission ratios at the grid point of Santiago of 19% for NO_X/CO and 200% for $NO_X/PM_{2.5}$, also departing from the values observed during PPE. In addition, residential heating by domestic combustion of wood and/or fossil fuel is expected to have slow variations in time, depending essentially on outside temperature (Saide et al., 2016), which as discussed above was not particularly colder on peak days than on other days, permitting to rule out residential heating as the main contribution to these short-lived peaks. Industrial emissions are also generally constant through time, excluding the possibility that they could be the main factor either. HTAP emission ratios for industry also significantly differ from the PPE situation, with 20% for NO_X/CO and 186% for $NO_X/PM_{2.5}$. Other sources than usual must then cause these peaks.
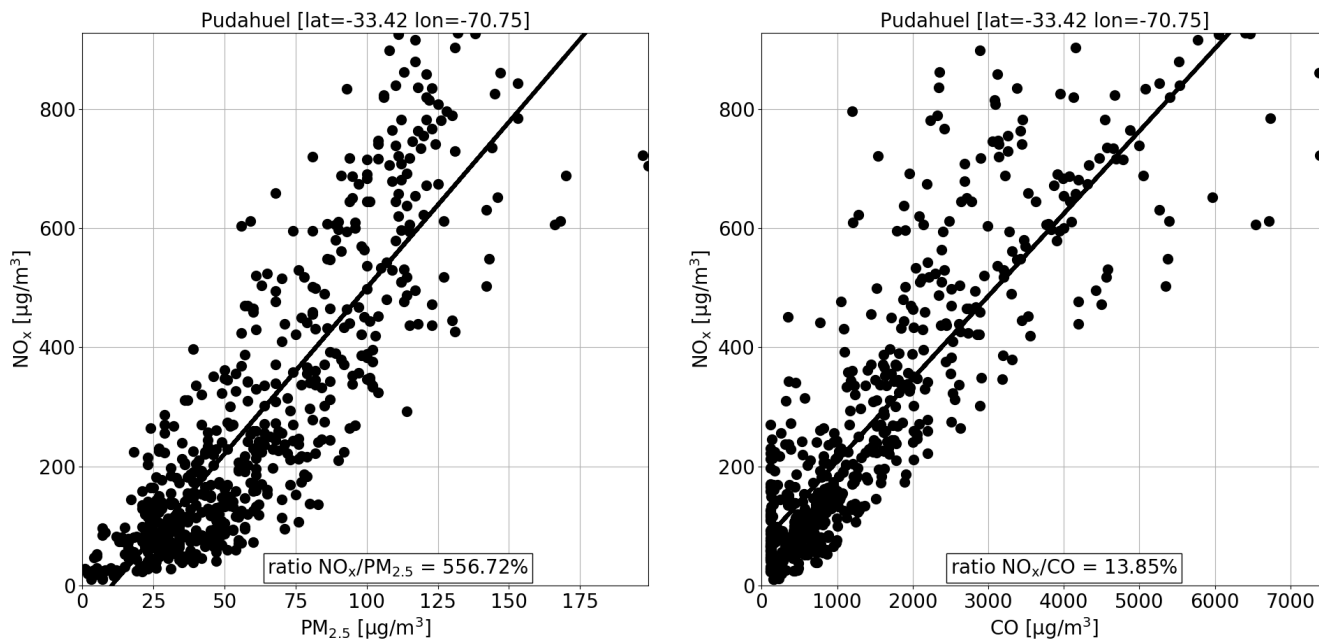
Figure 6. Pollutants ratios when no peak event occurs - July 2015 and 2016 - Pudahuel station

Since the peak events considered occurred exclusively during evenings/nights, cooking emissions such as barbecues, which are a cultural habit in Chile, could be a candidate. Different studies estimate emission factors from barbecue cooking (charcoal only and including meat emissions), from which ratios of 1.4% (Vicente et al., 2018) to 2.4% (Lee, 1999) for NO_X/CO and 40.5% (Vicente et al., 2018) to 61.5% (Lee, 1999) for $NO_X/PM_{2.5}$ can be derived. These numbers are not far from the 4.6% and 73% observed during PPE (Fig. 7), suggesting that, although the atmospheric composition is likely the result of multiple sources, the main signal in the observed $PM_{2.5}$ concentrations corresponds to emissions from barbecues. As a first order approximation, we use emission ratios and concentration ratios equivalently. This assumption is examined in Sect. 4. However, one question remains: why would there be peaks of barbecue cooking in the nights of June 18th and June 26th specifically, rather than other nights during the studied period? Even more so given that barbecues are mainly a spring-summer activity in Chile.

Usually, barbecues (or "asados") are cooked when celebrating particular events in Chile. So as to gain statistical significance by including more events, the time period studied is expanded to winter 2015 and 2014 as well. As it turns out, during the month of June of these three years, 8 episodes with hourly $PM_{2.5}$ higher than $200\mu g/m^3$ were recorded at Pudahuel station, 5 of which peaked during international soccer games involving the Chilean national team. The three others were declared within 24 hours after a game. It is even clearer for peaks higher than $400\mu g/m^3$, all of them occurring at the exact same hour as the kick-off of a soccer game when the next day is not a working day - see Fig. 8: red diamonds represent Chile games kick-off during the 2014 world cup, 2015 Copa América and 2016 Copa América. In addition, for the recent years without major soccer
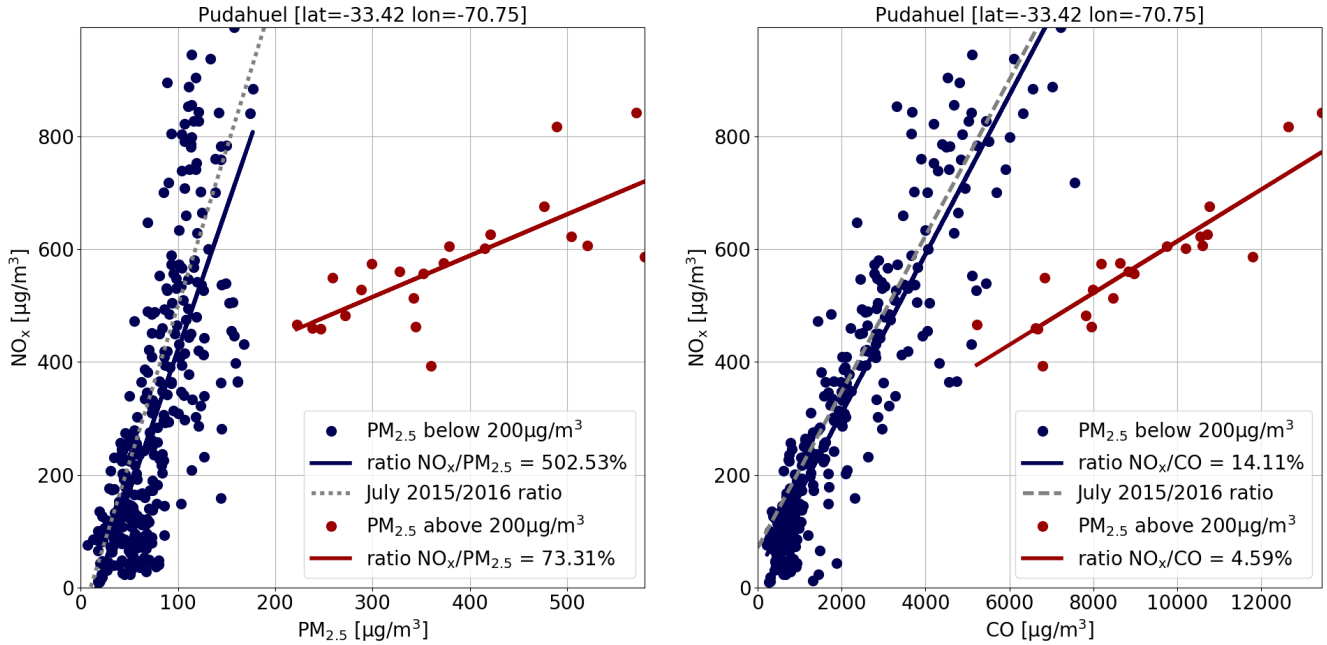
Figure 7. Observed NO_X/CO and $NO_X/PM_{2.5}$ concentration ratios at Pudahuel station (PDH). Blue dots are for $PM_{2.5}$ concentrations below $200\mu g/m^3$ - red dots are for $PM_{2.5}$ concentrations above $200\mu g/m^3$ - gray line represents the ratio for July 2015/2016 - blue and red lines correpond to linear regressions for each data set.

championship involving the team of Chile (i.e. 2010, 2012, 2013, 2017), the maximum hourly $PM_{2.5}$ concentration at Pudahuel over the same period of the year was $260\mu g/m^3$. In 2011 another Copa América was played and values reached up to $360\mu g/m^3$.

This correlation is likely not coincidental. Over the months of June 2014, 2015 and 2016, the observations show 12 days recording "pre-emergency" conditions (24-hour $PM_{2.5}$ concentration above $110\mu g/m^3$). Among these 12 days, 10 dates coincide with a soccer game of the national team or the day after such a game (games being played at nights, the peak affects both the game day and the day after). The 3 periods total 90 days, 15 of which were game days. Based on combinatorics, the probability that soccer games and $PM_{2.5}$ pre-emergency levels coincidentally occur with a proportion of at least 10 for 12 can be expressed as in Eq. (1). This corresponds to randomly drawing 15 days out of the 90 available, and obtaining at least 10 peaks. As a result, the probability that the correlation between $PM_{2.5}$ peaks and soccer games is purely coincidental is 0.002%. Thus we can be confident that there is actually a significant correlation between these two types of events, through massive barbecue cooking during games.

$$\mathbb{P}_{rand} = \frac{\binom{12}{10}\binom{78}{5} + \binom{12}{11}\binom{78}{4} + \binom{12}{12}\binom{78}{3}}{\binom{90}{15}} = 2.10^{-5} \tag{1}$$
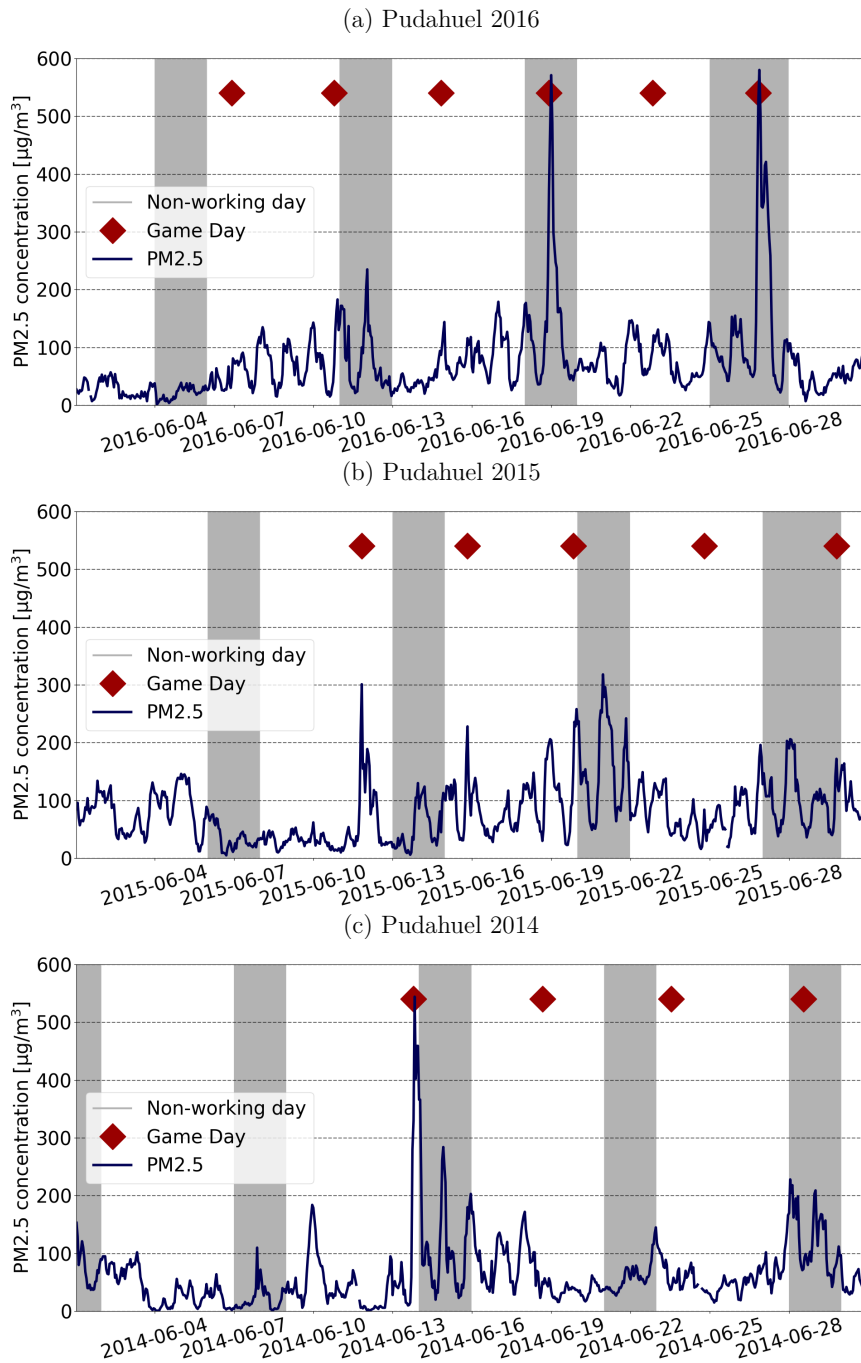
Figure 8. PM$_{2.5}$ peak events coincidence with soccer games. (a) Hourly PM$_{2.5}$ concentrations at Pudahuel monitoring station (solid blue line), kick-off hours of soccer games (red diamonds) and non-working days (gray shaded areas) - June 2016. (b) same as (a) for June 2015. (c) same as (a) for June 2014.

The observations made in Fig. 7 are also valid for other stations throughout the city. Figure 9 shows the NO_X/CO and NO_X/$PM_{2.5}$ ratios for three other locations in Santiago, distinguishing between the hours around the games of June 18th and June 26th (red dots), and the other data for the month (blue dots). Then again, two different regimes are observed, the one during games being attributable to barbecues based on the same analysis as previously done, although barbecues seem to be even more dominant in Pudahuel. In summary, we have shown here that major peak events of $PM_{2.5}$ in Santiago are correlated with soccer games played on the evening before a non-working day, and such conditions can be tied to massive barbecue cooking throughout the city, given the chemical footprint observed at that times.
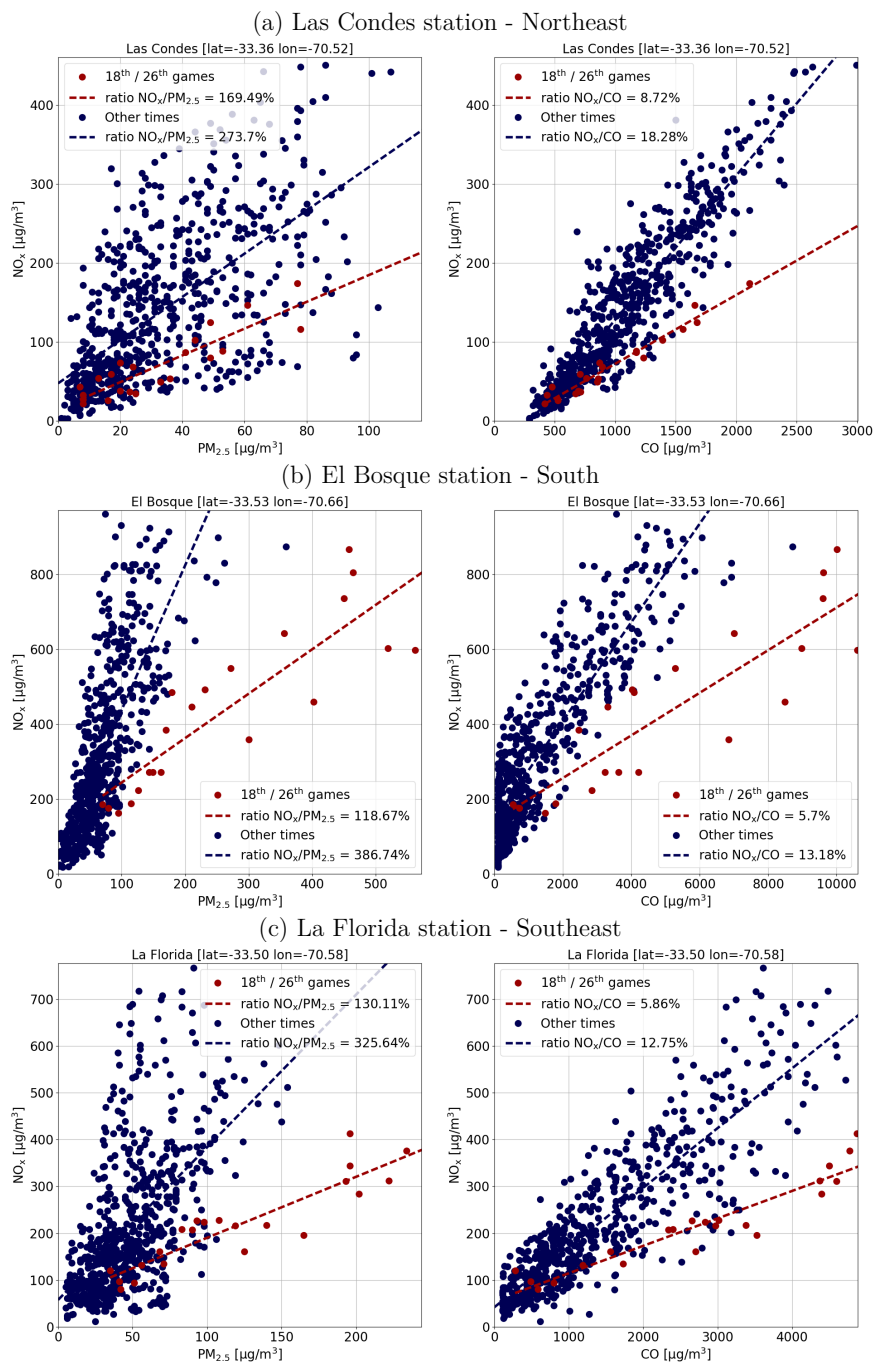
Figure 9. Observed NO_X/CO and $NO_X/PM_{2.5}$ concentration ratios at 3 stations in June 2016. Blue dots are observations during the June 18th and June 26th soccer games. Red dots correspond to the rest of the data. Blue and red dashed lines correpond to linear regressions for each case.

3.3 Transport

These barbecue peaks, although generating large amounts of $PM_{2.5}$, last only a few hours. The termination of one of these events
190 is studied hereafter. A chemistry-transport simulation is run with WRF (Skamarock et al., 2008) and CHIMERE (Mailler et al.,
2017) for the austral winter 2016 (see Section 2 for the details). A first baseline simulation aiming to reproduce observed con-
centrations of pollutants is performed using HTAP anthropogenic emissions inventory (Janssens-Maenhout et al., 2015). This
inventory does not account for sporadic emissions such as the ones studied here. Despite a good performance in reproducing
the observed meteorology and atmospheric composition (see Section 2, Tables 2, 3, 4), the model does not produce peak events
195 on June 18th and June 26th (dashed black line in Fig. 10). This reinforces the idea that strong sporadic emissions are actually at
play rather than extreme weather conditions. In a second simulation, all other things remaining equal, strong additional sources
of $PM_{2.5}$ are added all over the city based on population density, and plugged into CHIMERE in order to account for barbecues
being cooked on June 26th.

A survey conducted before the final game of the 2016 Copa América estimated that 29% of Santiago's inhabitants would
200 cook a barbecue during the game (Panel Ciudadano de la Universidad del Desarrollo, June 26th 2016). As a first order approx-
imation, considering only the adult population and assuming that this is a group activity gathering on average 7 people, we
estimate that this corresponds to 100,000 fires that were lit at the time of the game. Based on PM emission rates estimated by
the US Environmental Protection Agency (Lee, 1999) at around 20g/hr on average, with variations depending on the type of
meat cooked, the expected additional emission of $PM_{2.5}$ would be a total of 2 tons per hour for the whole region. In a heavily
205 populated area such as El Bosque, this represents an additional signal 15 times higher than the $PM_{2.5}$ emission rate used in the
baseline simulation. We acknowledge the multiple sources of uncertainty in this estimation. However our goal is to explore
barbecues as a potential significant source of $PM_{2.5}$ pollution, which only requires orders of magnitude given the strength of
the signal. Barbecues are assumed to last 3 hours starting 1 hour before the game kick-off. The estimated additional emissions
are plugged in CHIMERE for the peak simulation (gray line in Fig. 10).
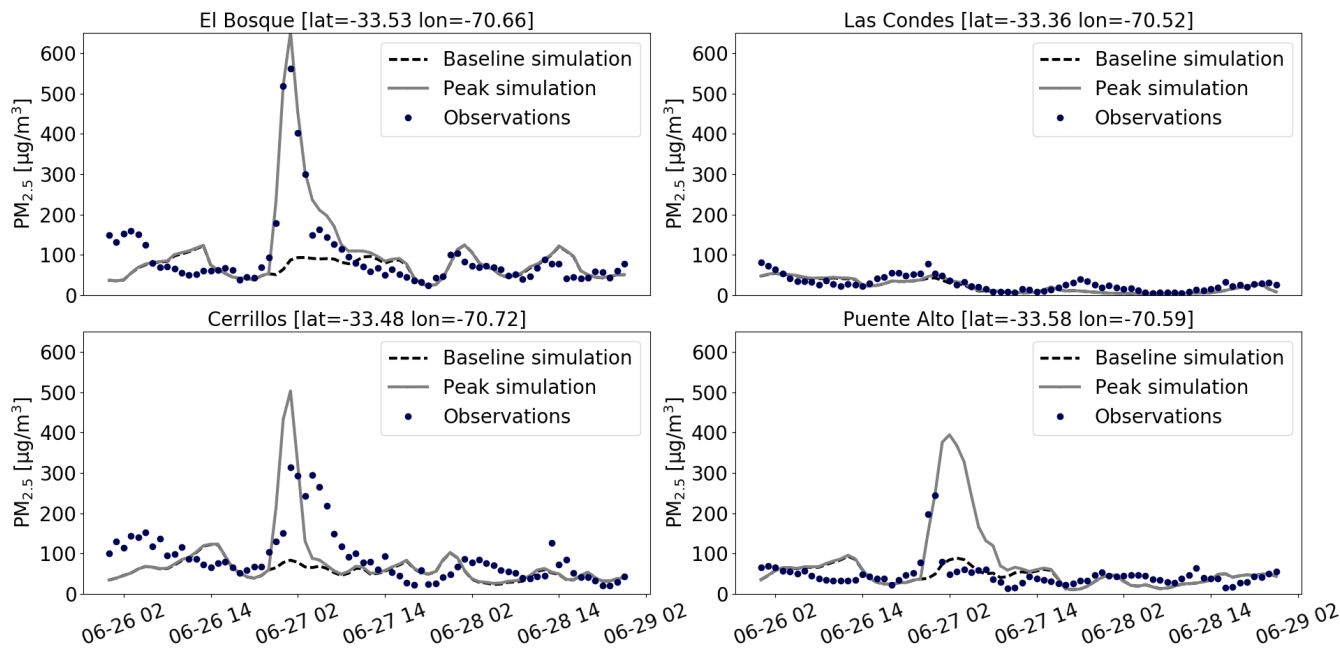
Figure 10. Observed (blue dots) and simulated (baseline simulation in black dashed line, peak simulation in gray) PM$_{2.5}$ surface concentrations time series at 4 stations in Santiago, around the peak episode of June 26th 2016

The resulting PM$_{2.5}$ concentration time series in Fig. 10 shows that the observations are well reproduced using this proxy in the South (El Bosque) and Northeast (Las Condes). Although the magnitude is a little overestimated but not far off, the time evolution of concentrations is less well reproduced in the West (Cerrillos) where the peak is too short, and in the Southeast (Puente Alto) where it lasts too long. This is possibly due to the representation of slope winds by the model: too weak easterlies coming from the Andes in the simulation would result in not enough ventilation in the East (i.e. a peak too long) and not enough accumulation in the West (i.e. a too short-lived event). Not many observations are available to investigate this hypothesis. Generally speaking, the peak simulation comforts the magnitude of our estimate of 100,000 barbecues cooked during the game, or an additional 6 tons of PM$_{2.5}$ emitted in total for the area.

Based on this simulation, the transport of the particles generated by the barbecue events can also be studied. Figures 11 and 12 show the difference in PM$_{2.5}$ concentration between the two simulations aforementioned, for the peaks on July 26th and July 18th, respectively. Concentrations at 60m above ground level are considered in order to get rid of the signal of emissions. The simulations result in an evacuation of the particles towards the Southwest of Santiago for both events, a few hours after the onset. Then again the episodes are short-lived in the city, but have impacts on adjacent areas several hours later and several kilometers away from the emission site. For both events the areas impacted by the dispersion of the plume are the South and Southwest regions. Although this result is consistent with mountain-valley circulation, it does not imply that such a dispersion pattern is the only one that can occur during peak events. In addition to the impact within the city, collateral effects outside

Santiago must be studied in greater detail, such as a potential deposition of the particles on crops, with effects on yields, or adjacent glaciers, with radiative effects.
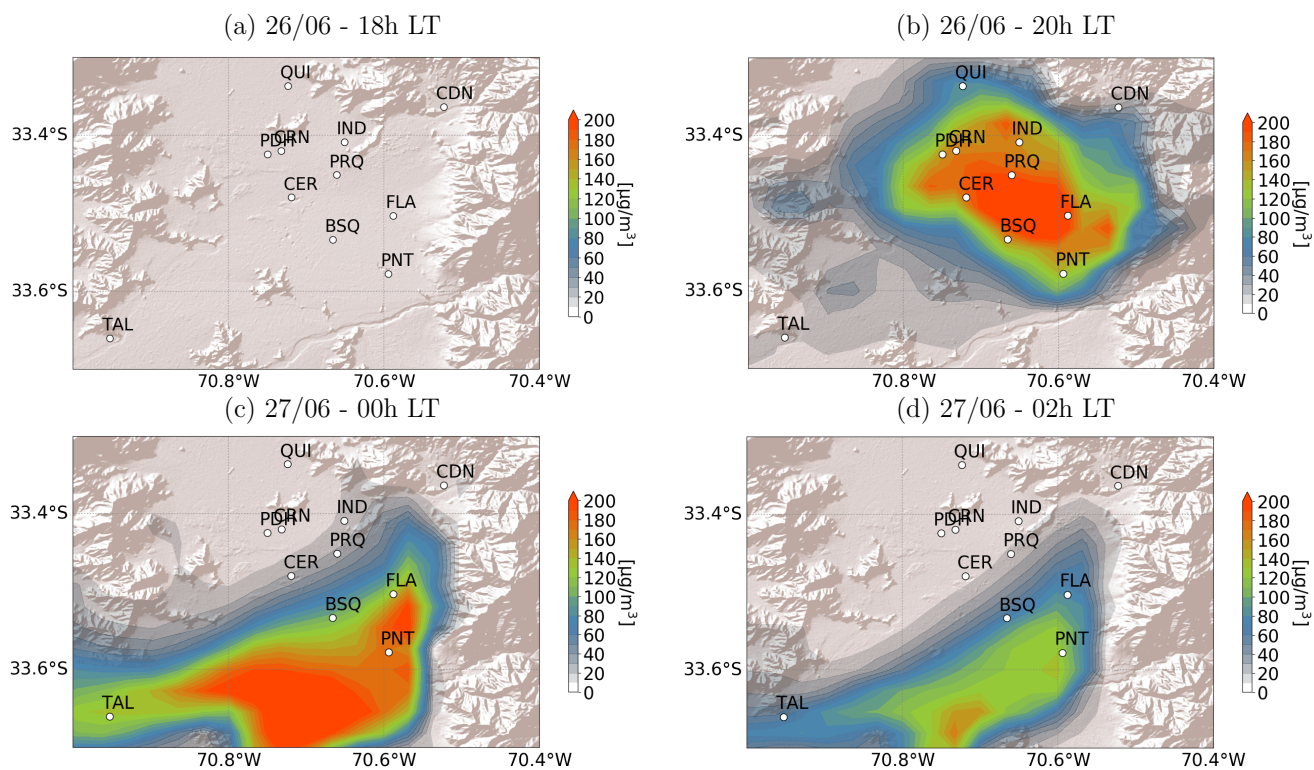
Figure 11. PM$_{2.5}$ concentration difference at 60m above surface between the peak event and baseline simulation in June 26th/27th. Positive values indicate excess concentrations in the peak event scenario compared to baseline. Map background layer: World Shaded Relief, ©2009 ESRI.
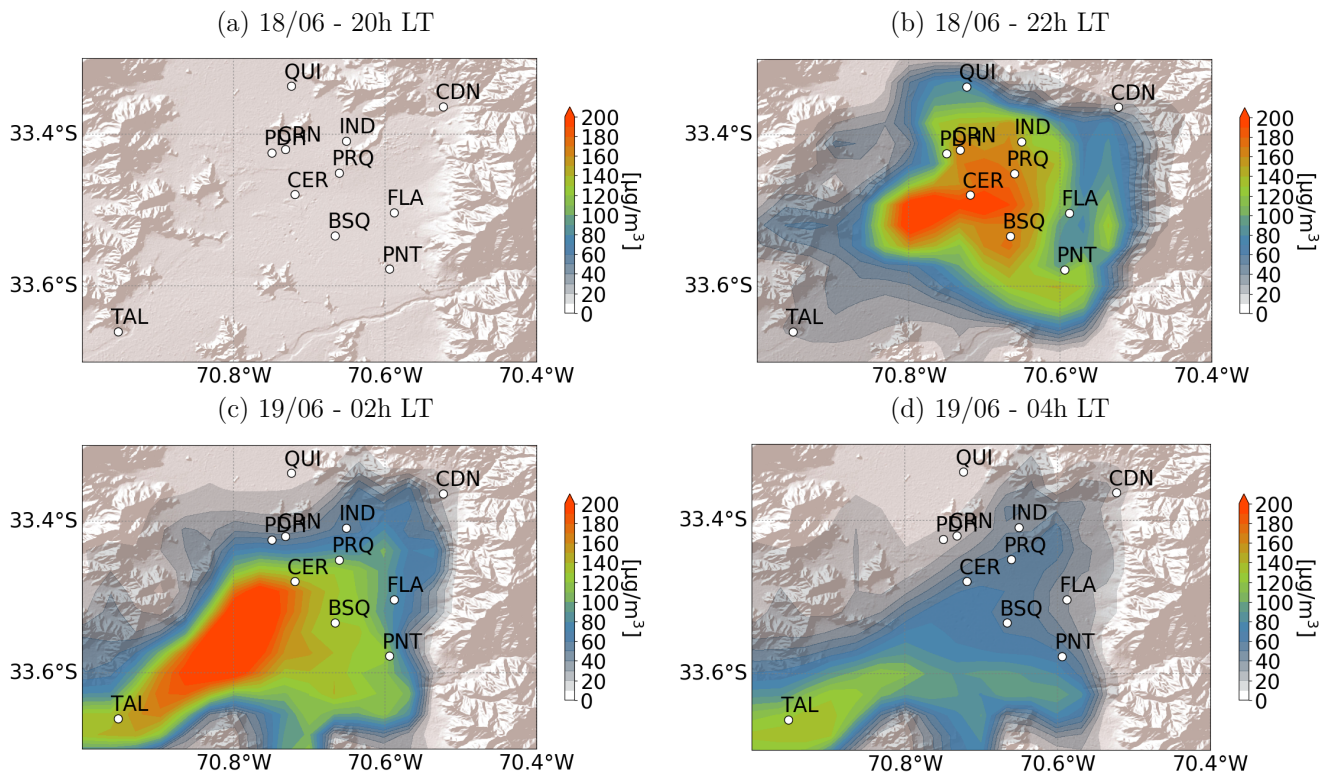
Figure 12. PM$_{2.5}$ concentration difference at 60m above surface between the peak event and baseline simulation in June 18th/19th. Positive values indicate excess concentrations in the peak event scenario compared to baseline. Map background layer: World Shaded Relief, ©2009 ESRI.

4 Discussion

In Sect. 3.2, the conclusions are based on the approximation that the concentration ratios observed correspond to the ratios
230 of the underlying emission factors. Chemical processes are at play in the atmosphere that can lead to a difference between these two variables though. However atmospheric lifetimes of NO$_X$ and CO (respectively 1 to 10 days and 1 to 4 months (Seinfeld and Pandis, 2006)) are too long for these species to be significantly removed during the few hours we focus on. The NO$_X$/CO ratio at emission and concentration ratio are thus expected to be very close. For particulate matter, the discussion is less clear. Secondary PM can form, adding to the emitted PM$_{2.5}$. The nucleation of secondary PM would lead to a NO$_X$/PM$_{2.5}$
235 concentration ratio smaller than the emission ratio. However, one order of magnitude separates the two regimes we observe, and the time scale we study does not leave much time for secondary PM to become significant, implying a small contribution to the total PM (for instance the apportionment of secondary versus primary aerosols in our baseline simulation varies between 4% and 63% with an average value of 33%).

5 Conclusions

In the last decades, decontamination plans in Santiago have mainly focused on decreasing traffic, industrial and residential heating emissions. The chemical footprint of extreme peak events evidenced in this study advocates in favor of also considering more specific and sporadic sources based on cultural habits such as barbecues. Indeed, the mitigation policies currently implemented are helping lowering pollution levels, but based on our study, cannot prevent extreme $PM_{2.5}$ events from happening while their impact can be significant as well. The "game effect" phenomenon has been hypothesized by local authorities but had not been backed up by scientific evidence so far. An analysis of the time characteristics of the events showed that they happen exclusively during soccer games of the national team, played in evenings before a non-working day. The observed concentrations of NO_X, CO and $PM_{2.5}$ at that times, compared with the usual levels, allow to trace back the main contribution to fine particles emitted by barbecue cooking. The amount of barbecues cooked during one peak event is estimated and the associated emissions are plugged into a chemistry-transport simulation, leading to the reproduction of the observed peaks, which is not the case without these emissions. The model then yields appropriate levels, thus comforting the estimated emissions, and allowing to study the evacuation of the $PM_{2.5}$ plume towards the Southwest of the metropolitan area. The more general question of the fate and impacts of particulate matter plumes generated in Santiago is raised.

Although the results provided here seem to have geographically limited implications, the general methodology can be reproduced and benefit to other places in the world. Indeed, using only a limited set of data, with no speciation of particulate matter, already enables to conclude on the source of extreme events, provided they are tied to cultural habits differing from the usual sources of air pollution. Such type of sporadic habits are usually ignored by air quality plans implemented by cities, due to the lack of scientific evidence.

In addition, a model-based approach allowed to constrain the estimate of number of barbecues cooked during the final game of the 2016 Copa América (around 100,000). Not only this result can have an informative value for local authorities, but such a sensitivity analysis can be reproduced and applied to other cases throughout the world in order to estimate the burden on air quality of specific sources.

Code availability. The CHIMERE model used can be found at http://www.lmd.polytechnique.fr/chimere/CW-download.php. The WRF model used can be found at http://www2.mmm.ucar.edu/wrf/users/download/get_source.html.

Data availability. Surface observation data used in this study are available at https://sinca.mma.gob.cl/index.php/region/index/id/M. HTAP raw emission inventory can be downloaded at http://edgar.jrc.ec.europa.eu/htap_v2/. Other data can be made available from the corresponding author upon reasonable request.

Author contributions. N. Huneeus provided meteorological profiles data and synoptic stations wind speeds used to assess the quality of the simulation. As developers of CHIMERE, L. Menut and S. Mailler supervised the chemistry transport simulations and analyses of the results. R. Lapere performed the data analysis and model simulations, and coordinated the writing of the paper with L. Menut, S. Mailler and N.
270   Huneeus.

Competing interests. The authors declare that they have no conflict of interest.

Acknowledgements. N. Huneeus acknowledges the projects FONDECYT Regular 1181139 and FONDAP 15110009. The authors are grateful to Ricardo C. Muñoz for providing us with the ceilometer backscatter profiles and mixed layer height computations used in the meteorological analysis. The authors wish to thank the two anonymous reviewers for their constructive comments during the discussion phase.

References

Barraza, F., Lambert, F., Jorquera, H., Villalobos, A. M., and Gallardo, L.: Temporal evolution of main ambient $PM_{2.5}$ sources in Santiago, Chile, from 1998 to 2012, Atmos. Chem. Phys., 17, 10 093–10 107, https://doi.org/10.5194/acp-17-10093-2017, 2017.

de la Barrera, F., Barraza, F., Favier, P., Ruiz, V., and Quense, J.: Megafires in Chile 2017: Monitoring multiscale environmental impacts of burned ecosystems, Sci. Total Environ., 637-638, 1526–1536, https://doi.org/10.1016/j.scitotenv.2018.05.119, 2018.

Energy Policy Institute at the University of Chicago: Air Quality Life Index, https://aqli.epic.uchicago.edu/, 2017.

Gallardo, L., Barraza, F., Ceballos, A., Galleguillos, M., Huneeus, N., Lambert, F., Ibarra, C., Munizaga, M., O'Ryan, R., Osses, M., Tolvett, S., Urquiza, A., and Véliz, K. D.: Evolution of air quality in Santiago: The role of mobility and lessons from the science-policy interface, Elem. Sci. Anth., 6, 38, https://doi.org/10.1525/elementa.293, 2018.

Ilabaca, M., Olaeta, I., Campos, E., Villaire, J., Tellez-Rojo, M. M., and Romieu, I.: Association between Levels of Fine Particulate and Emergency Visits for Pneumonia and other Respiratory Illnesses among Children in Santiago, Chile, J. Air Waste Manage., 49, 154–163, https://doi.org/10.1080/10473289.1999.10463879, 2011.

Instituto Nacional de Estadísticas: Anuarios Parque de Vehiculos en Circulacion, http://historico.ine.cl/canales/chile_estadistico/estadisticas_economicas/transporte_y_comunicaciones/parquevehiculos.php, 2016.

Janssens-Maenhout, G., Crippa, M., Guizzardi, D., Dentener, F., Muntean, M., Pouliot, G., Keating, T., Zhang, Q., Kurokawa, J., Wankmüller, R., Denier van der Gon, H., Kuenen, J. J. P., Klimont, Z., Frost, G., Darras, S., Koffi, B., and Li, M.: HTAP_v2.2: a mosaic of regional and global emission grid maps for 2008 and 2010 to study hemispheric transport of air pollution, Atmos. Chem. Phys., 15, 11 411–11 432, https://doi.org/10.5194/acp-15-11411-2015, 2015.

Lee, S. Y.: Emissions from street vendor cooking devices (charcoal grilling), Tech. rep., United States Environmental Protection Agency, 1999.

Mailler, S., Menut, L., Khvorostyanov, D., Valari, M., Couvidat, F., Siour, G., Turquety, S., Briant, R., Tuccella, P., Bessagnet, B., Colette, A., Létinois, L., Markakis, K., and Meleux, F.: CHIMERE-2017: from urban to hemispheric chemistry-transport modeling, Geosci. Model Dev., 10, 2397–2423, https://doi.org/10.5194/gmd-10-2397-2017, 2017.

Mazzeo, A., Huneeus, N., Ordoñez, C., Orfanoz-Cheuquelaf, A., Menut, L., Mailler, S., Valari, M., van der Gon, H. D., Gallardo, L., Muñoz, R., Donoso, R., Galleguillos, M., Ossesa, M., and Tolvett, S.: Impact of residential combustion and transport emissions on air pollution in Santiago during winter, Atmos. Environ., 190, 195–208, https://doi.org/10.1016/j.atmosenv.2018.06.043, 2018.

Menut, L., Bessagnet, B., Khvorostyanov, D., Beekmann, M., Blond, N., Colette, A., Coll, I., Curci, G., Foret, G., Hodzic, A., Mailler, S., Meleux, F., Monge, J.-L., Pison, I., Siour, G., Turquety, S., Valari, M., Vautard, R., and Vivanco, M. G.: CHIMERE 2013: a model for regional atmospheric composition modelling, Geosci. Model Dev., 6, 981–1028, https://doi.org/10.5194/gmd-6-981-2013, 2013.

Ministerio del Medio Ambiente: Análisis General para el Impacto Económico y Social (AGIES) de la Norma de Calidad Primaria de Material Particulado 2.5, Tech. rep., MMA, http://planesynormas.mma.gob.cl/archivos/2014/proyectos/235_6__Folio_N_881_al_1008.pdf, 2012.

Ministerio del Medio Ambiente: Establece Plan de Prevención y Descontaminación Atmosférica para la Región Metropolitana de Santiago, https://www.leychile.cl/N?i=1111283&f=2017-11-24&p=, 2017.

Ministerio del Medio Ambiente: Sistema de Información Nacional de Calidad del Aire, https://sinca.mma.gob.cl/index.php/, 2018.

Muñoz, R. C. and Undurraga, A. A.: Daytime Mixed Layer over the Santiago Basin: Description of Two Years of Observations with a Lidar Ceilometer, J. Appl. Meteorol. Clim., 49, 1728–1741, https://doi.org/10.1175/2010JAMC2347.1, 2010.

NCEP: NCEP FNL Operational Model Global Tropospheric Analyses, continuing from July 1999, https://doi.org/10.5065/D6M043C6, 2000.

Panel Ciudadano de la Universidad del Desarrollo: Santiaguinos esperan con altas expectativas el partido de hoy... y un 29% hará asado, El Mercurio, https://gobierno.udd.cl/cpp/noticias/2017/01/17/santiaguinos-esperan-con-altas-expectativas-el-partido-de-hoy-y-un-29-hara-asado/, June 26th 2016.

315 Petit, J.-E., Amodeo, T., Meleux, F., Bessagnet, B., Menut, L., Grenier, D., Pellan, Y., Ockler, A., Rocq, B., Gros, V., Sciare, J., and Favez, O.: Characterising an intense PM pollution episode in March 2015 in France from multi-site approach and near real time data: Climatology, variabilities, geographical origins and model evaluation, Atmos. Environ., 155, 68–84, https://doi.org/10.1016/j.atmosenv.2017.02.012, 2017.

Rubio, M. A., Lissi, E., Gramsch, E., and Garreaud, R. D.: Effect of Nearby Forest Fires on Ground Level Ozone Concentrations in Santiago,
320 Chile, Atmosphere, 6, 1926–1938, https://doi.org/10.3390/atmos6121838, 2015.

Rutllant, J. and Garreaud, R.: Meteorological Air Pollution Potential for Santiago, Chile: Towards an Objective Episode Forecasting, Environ. Monit. Assess., 34, 223–244, https://doi.org/10.1007/BF00554796, 1995.

Saide, P. E., Mena-Carrasco, M., Tolvett, S., Hernandez, P., and Carmichael, G. R.: Air quality forecasting for winter-time $PM_{2.5}$ episodes occurring in multiple cities in central and southern Chile, J. Geophys. Res. Atmos., 121, 558–575, https://doi.org/10.1002/2015JD023949,
325 2016.

Seinfeld, J. H. and Pandis, S. N.: Atmospheric Chemistry and Physics: From Air Pollution to Climate Change. Second Edition., John Wiley & Sons, Inc., Hoboken, New Jersey, 2006.

Shaiganfar, R., Beirle, S., Denier van der Gon, H., Jonkers, S., Kuenen, J., Petetin, H., Zhang, Q., Beekmann, M., and Wagner, T.: Estimation of the Paris NO_x emissions from mobile MAX-DOAS observations and CHIMERE model simulations during the MEGAPOLI campaign
330 using the closed integral method, Atmos. Chem. Phys., 17, 7853–7890, https://doi.org/10.5194/acp-17-7853-2017, 2017.

Skamarock, W. C., Klemp, J. B., Dudhia, J., Gill, D. O., Barker, D. M., Duda, M. G., Huang, X.-Y., Wang, W., and Powers, J. G.: A Description of the Advanced Research WRF Version 3, NCAR Technical Note, 27, 2008.

Toledo, F., Garrido, C., Díaz, M., Rondanelli, R., Jorquera, S., and Valdivieso, P.: AOT Retrieval Procedure for Distributed Measurements With Low-Cost Sun Photometers, J. Geophys. Res. Atmos., 123, 1113–1131, https://doi.org/10.1002/2017JD027309, 2018.

335 Toro A, R., Kvakić, M., Klaić, Z. B., Koračin, D., Morales S, R. G., and Leiva G, M. A.: Exploring atmospheric stagnation during a severe particulate matter air pollution episode over complex terrain in Santiago, Chile, Environ. Pollut., 244, 705–714, https://doi.org/10.1016/j.envpol.2018.10.067, 2018.

University of Maryland: GLCF: MODIS Land Cover, http://glcf.umd.edu/data/lc/, 2010.

Vicente, E., Vicente, A., Evtyugina, M., Carvalho, R., Tarelho, L., Oduber, F., and Alves, C.: Particulate and gaseous emissions from charcoal
340 combustion in barbecue grills, Fuel Process. Technol., 176, 296–306, https://doi.org/10.1016/j.fuproc.2018.03.004, 2018.

World Health Organization: WHO Air quality guidelines for particulate matter, ozone, nitrogen dioxide and sulfur dioxide : global update 2005 : summary of risk assessment, 2006.

WRF configuration		CHIMERE configuration	
Coarse domain resolution	15km	Coarse domain resolution	15km
Nested domain resolution	3km	Nested domain resolution	3km
Microphysics	WSM3	Chemistry	MELCHIOR
Boundary and surface layer	MYNN	Gas/Aerosol Partition	ISORROPIA
Land surface	Noah LSM	Horizontal Advection	Van Leer
Cumulus parameterization	Grell G3	Vertical Advection	Upwind
Longwave radiation	CAM	Boundary Conditions	LMDz-INCA + GOCART
Shortwave radiation	Dudhia		

Table 1. WRF and CHIMERE configurations.

Station:	El Bosque				Independencia		
	MB	NRMSE	R		MB	NRMSE	R
TEMP	1.3	0.34	0.84	:	-1.06	0.2	0.86
RH	-12.7	0.30	0.62	:	-16.6	0.31	0.7
WS	-0.08	0.42	0.56	:	0.23	1.29	0.7

Table 2. Simulation scores for low-level meteorology. June 15th to July 15th 2016

Day:	June 27th 2016				June 28th 2016				June 29th 2016		
	MB	RMSE	R		MB	RMSE	R		MB	RMSE	R
TEMP	-0.79	2.01	0.99	:	0.51	1.1	0.99	:	0.83	2.4	0.95
RH	7.64	14.3	0.80	:	-1.04	5.88	0.67	:	-7.47	22.2	0.82
WS	-1.92	3.54	0.39	:	1.06	2.71	0.84	:	-3.63	4.38	0.99
WD	-2	4	0.34	:	-4	82	0.71	:	19	85	0.48

Table 3. Simulation scores for meteorological vertical profiles for 3 days at DMC station in Santiago.

Network	PM$_{2.5}$		
	MB	NRMSE	R
La Florida	-0.45	0.55	0.63
Las Condes	3.31	0.62	0.62
Puente Alto	-3.26	0.72	0.45

Table 4. Simulation scores for low-level PM$_{2.5}$ concentrations. June 28th to July 15th 2016